

Transmission of slow highly charged ions through glass capillaries: Role of the capillary shape

C. L. Zhou,¹ M. Simon,² T. Ikeda,^{3,*} S. Guillois,¹ W. Iskandar,¹ A. Méry,¹ J. Rangama,¹ H. Lebius,¹ A. Benyagoub,¹ C. Grygiel,¹ A. Müller,² M. Döbeli,² J. A. Tanis,^{1,4} and A. Cassimi¹

¹*CIMAP/CIRIL, CEA/CNRS/ENSICAEN, Boîte Postale 5133, F-14070 Caen cedex 5, France*

²*ETH Swiss Federal Institute of Technology, 8092 Zurich, Switzerland*

³*Atomic Physics Laboratory, RIKEN, 2-1 Hirosawa, Wako, Saitama 351-0198, Japan*

⁴*Department of Physics, Western Michigan University, Kalamazoo, Michigan 49008, USA*

(Received 4 August 2013; published 27 November 2013)

Comparison of the transmission of 27-keV Ar⁹⁺ ions through insulating funnel- and conical-shaped glass capillaries of outlet diameters of $\sim 22 \mu\text{m}$ is reported. Beam intensities of 1, 5, and 10 pA were injected into both capillaries. Transmission at the untilted angle of 0° was measured as well as at a tilt angle of $\sim 0.5^\circ$ for the funnel capillary and a tilt angle of $\sim 1.1^\circ$ for the conical capillary. For the funnel capillary, blocking of transmission was observed, whereas, the transmission was continuous for the conical capillary. These measurements suggest that conical-shaped capillaries have transport properties that are different than funnel-shaped capillaries for slow highly charged ions.

DOI: [10.1103/PhysRevA.88.050901](https://doi.org/10.1103/PhysRevA.88.050901)

PACS number(s): 61.85.+p, 34.50.Fa, 34.35.+a

In the past decade, considerable work has been devoted to studying slow highly charged ion (HCI) transmission through insulating capillaries [1–7]. These studies are aimed at both the fundamental aspect of ion-surface interactions as well as the challenge of manipulating particles for surface modifications [1]. The pioneering work referred to as “guiding”, proposed by the group of Stolterfoht *et al.* in 2002 [2], showed that nearly all of the slow HCIs (3-keV Ne⁷⁺) passing through insulating nanocapillaries formed in polyethylene terephthalate (PET) foils keep their incident charge state and incident energy even for tilt angles up to 25° . This is sharply in contrast with the previous metal capillary experiments for which only hollow atoms and transmission within the opening angle of capillaries were observed [8]. The guiding mechanism for insulating capillaries was attributed to the charge deposited on the inner walls by the initial ions incident on the capillary, hence, allowing the following ions to be guided towards the exit. The guiding angle has been defined as the tilt angle for which the transmitted intensity decreases by a factor of $1/e$ compared to the aligned capillary intensity. This guiding could, thus, provide a way to manipulate slow HCIs by capillaries. Up to now, the guiding effect has been investigated extensively for slow heavy ions striking various capillary materials, such as PET [2], Al₂O₃ [3], SiO₂ [4], polycarbonate [5], and Pyrex glass [1,6,7]. Experiments have also been performed with other particles including fast electrons [9,10] and muons [11], showing similar results.

A microbeam of slow HCI using the guiding effect was first achieved with an individual funnel-shaped capillary (referred to as a tapered capillary in that paper) having a beam size of $\sim 24 \mu\text{m}$ [1]. It was found that incoming intensities up to 0.3 pA achieved a focusing factor, defined as the ratio of outgoing beam density to the incoming beam density of ~ 10 . Nevertheless, a blocking effect was observed for higher intensities of ~ 0.33 – 0.44 pA for a $50\text{-}\mu\text{m}$ funnel-shaped

capillary [12]. Even for cylindrical multiple nanocapillary foils, blocking was observed for 3-keV Ne⁷⁺ [5]. It should be noted that ion transmission has also been observed through macroscopic cylindrical capillaries with diameters of $170 \mu\text{m}$ [6]. The mechanism of transmission and blocking requires further study to better understand these effects.

In order to investigate the origin of the blocking phenomenon, we concentrate on not only the input intensity, but also the shape of the glass capillaries. The study for the shape dependence of the transmission has only been reported for simulations [13], whereas, the blocking has not yet been studied. To parametrize the wall shape of funnel-shaped glass capillaries is very complicated because the taper angle is not constant along the capillary axis (the funnel shape). This is the reason why such studies have not shown much progress. However, capillaries with ideal shapes have been newly developed [14], whose taper angles are constant along the capillary axis (conical shape). Our aims are to compare the transmission characteristics of slow HCIs between the funnel and the conical shapes and to obtain knowledge about the origin of the blocking. In this way, it is hoped to contribute to provide better transmission capillaries applicable to fields using microbeam irradiation in vacuum.

In this Rapid Communication, both the nearly ideal conical-shaped glass capillary and the funnel-shaped capillary were used in the experiments (Fig. 1). (Note: Funnel-shaped capillaries have previously been referred to as tapered capillaries. Since both funnel-shaped and conical-shaped capillaries are tapered, it is better to distinguish them in the way performed in this Rapid Communication.)

It was found that the conical-shaped capillary transmitted 27-keV Ar⁹⁺ ions for different injected beam intensities ranging from ~ 1 to 10 pA, whereas, the funnel-shaped capillary blocked transmission after a sufficient charge was inserted. These capillaries are similar in that they are made of the same material and have nearly the same inlet and outlet dimensions as well as length with only a difference in the shape. The beam energy and charge state were chosen to ensure that guiding would occur based on results for similar studies

*Present address: RIKEN Nishina Center for Accelerator-Based Science, 2-1 Hirosawa, Wako, Saitama 351-0198, Japan.



FIG. 1. (Color online) Pictures of the capillaries used in the experiment: (a) funnel-shaped capillary and (b) conical capillary.

with both micrometer- and nanometer-sized capillaries (see Refs. [1–7]). The elapsed time for transmission to occur in both capillaries, with a tilt angle up to $\sim 0.5^\circ$ for the funnel capillary and up to $\sim 1.1^\circ$ for the conical capillary, was measured and is presented. Transmission also was obtained after a delay time of a few minutes for the conical capillary at a tilt angle of $\sim 1.8^\circ$, whereas, no beam transmission was observed for tilt angles beyond 1° for the funnel capillary in the present measurements.

Despite similarities in the physical characteristics of the two samples (same material, inlet and outlet diameters, and length), the behavior of highly charged ion transmission through each capillary shape is very different. It is expected that this difference in the transmission of the two capillaries will lead to new insights into the behavior of ion interactions with the walls of the capillaries as well as ideas for the applications of the capillaries, particularly, in the areas of biological and medical uses.

The experiments were carried out with 27-keV Ar^{9+} ions from the 14.5-GHz electron cyclotron resonance ion source at the ARIBE beamline of the GANIL facility (Caen, France). The capillaries were mounted behind two metal masks, which collimated the beam with apertures of diameters of ~ 3 and 0.6 mm in front of each capillary. The capillaries were coated on the front face with silver paint to provide an electrical contact with the 0.6-mm metal mask in order to avoid charge up at the entrance. The injected beam intensity was monitored by two picoammeters, each of which was connected in a series between each mask and ground [15], thus, determining the electric currents on the two masks. A multiple target holder was fixed on a goniometer having two translational degrees of freedom with an accuracy of $1 \mu\text{m}/\text{step}$ and two rotations with accuracies of $0.01^\circ/\text{step}$. A two-dimensional (2D) position-sensitive detector was installed 650 mm downstream of the goniometer rotation axis in the detector chamber. The incoming angular divergence was found to be about $\pm 0.34 \text{ mrad}$ ($\pm 0.02^\circ$) by measuring the beam profile through an $\sim 10\text{-}\mu\text{m}$ aperture placed on the target holder. More details on the experimental apparatus are presented elsewhere [15]. The vacuum in the target and detector chambers was better than 1×10^{-6} and 1×10^{-7} mbar, respectively. The data acquisition system recorded the events in “list mode” so off-line analysis could be achieved conveniently within the ROOT analysis framework [16].

Both capillaries (Fig. 1) are made of borosilicate glass (80.9% SiO_2 ; 12.7% B_2O_3 ; 2.3% Al_2O_3 ; $\text{Na}_2\text{O}/\text{K}_2\text{O}$) with a softening point of $\sim 821^\circ\text{C}$ and a volume resistivity of $\sim 10^{17} \Omega \text{ m}$. The funnel-shaped capillary has an inner entrance diameter of $\sim 800 \mu\text{m}$, an exit diameter of $\sim 23 \mu\text{m}$, a stretched

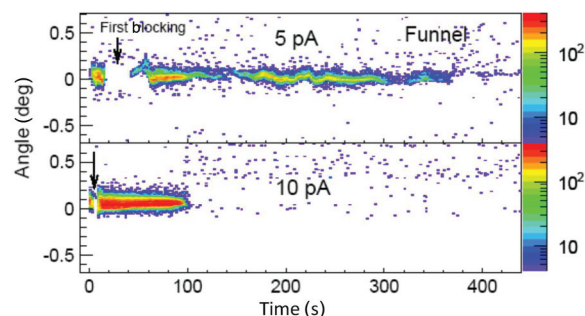


FIG. 2. (Color online) Evolution of the angular distribution of the incident beam measured as a function of time (charge) for the funnel-shaped capillary at a tilt angle of 0° . The first blocking is indicated by the arrow in each graph. The beam intensities are as indicated.

length of ~ 27 mm, a funnel length of ~ 4 mm, and a full length of ~ 80 mm [7]. The conical-shaped capillary was produced with an inner entrance diameter of $\sim 860 \mu\text{m}$, an exit diameter of $\sim 22 \mu\text{m}$, a full length of ~ 77 mm, and a cone angle of $\sim 0.3^\circ$. The funnel-shaped capillaries were made at the RIKEN Atomic Physics Laboratory in Wako, Japan, whereas, the conical capillaries were made at the ETH Laboratory in Zurich, Switzerland.

The angular distributions as a function of time for the $\sim 23\text{-}\mu\text{m}$ funnel capillary at a 0° tilt angle are presented in Fig. 2 for each of the beam intensities measured. These distributions correspond to the projection of the 2D position-sensitive detector images on the axis along which the capillary later was tilted. The beam was set onto the capillary after allowing sufficient time to discharge the sample, about 18 h before each measurement. The data were acquired for intensities of 5 pA (upper panel) and 10 pA (lower panel).

The behavior observed in Fig. 2 shows that the beam is blocked for both injected beam intensities after a certain time. To ensure that the beam was totally blocked, the measurements were carried out for another 800 s (not shown) for 5 pA and 700 s for 10 pA, respectively. Thus, the first blocking occurs at a deposited charge of ~ 70 pC for an intensity of 5 pA and at a deposited charge of ~ 40 pC for an intensity of 10 pA. The fact that the deposited charge of the first blocking is more (70 pC) for 5 pA, whereas, it is less (40 pC) for 10 pA is likely due to the charge diffusion that occurs with time. The upper plot for 5 pA shows several partial blockings and noticeable oscillations. In contrast, for an intensity of 10 pA, the transmission is relatively stable after the first blocking, until the transmission stops suddenly as blocking occurs after about 100 s.

Figure 3 shows the smooth transmission of the angular distributions, which only vary slightly with time, for the $\sim 22\text{-}\mu\text{m}$ conical capillary at a 0° tilt angle. The stable transmissions were obtained for the same beam intensities as those used for the funnel-shaped capillary shown in Fig. 2. The elapsed time before stable transmission occurs decreases as the input intensity increases with values of ~ 1000 s for the intensity of 1 pA, ~ 400 s for the intensity of 5 pA, and ~ 200 s for the intensity of 10 pA. Variations in the full width at half maximum (FWHM), as a function of time corresponding to the conical capillary, are plotted in Fig. 4. The width of the

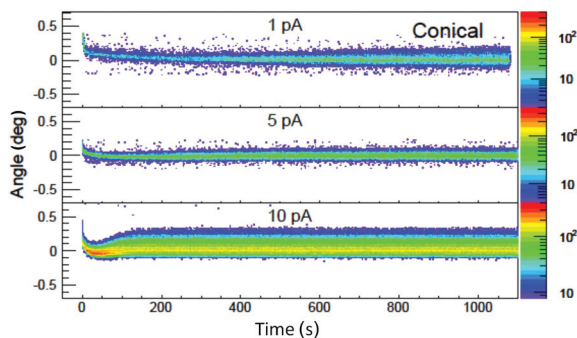


FIG. 3. (Color online) Evolution of the angular distribution of the incident beam measured as a function of time (charge) for the conical-shaped capillary at a tilt angle of 0° . The beam intensities are as indicated.

beam for 10 pA is wider than for the other two currents, which also can be seen directly from Fig. 3.

At the tilt angle of 0° shown in Fig. 3, the oscillation in the angular distribution mean value can be attributed to asymmetric charge up on the inner wall. This implies that the capillary axis and the beam are misaligned slightly due to small beam instabilities or to slight deviations from straightness of the capillary. Such a misalignment does not affect our conclusions, however. The width, as seen in Fig. 4, increases with time (deposited charge) and achieves a stable value after the equilibrium transmission is established. This is an indication that charge buildup at the exit of the capillary is responsible for the width broadening [5].

The measurements shown in Figs. 2 and 3 were repeated, and the same transmission patterns were observed. However, this is true only if complete discharging is achieved before each measurement and if neither the beam direction and intensity nor the capillary angle have been changed.

Considering that stable transmission in a funnel capillary can be maintained continuously for low intensities [1,12], the blocking effect found in this experiment is attributed to the relatively high beam intensity and the funnel-shaped part of the capillary. In this case, the high intensity incident on the funnel capillary portion corresponds to angles between the capillary walls and the ion trajectories, which are too large to allow ion guiding.

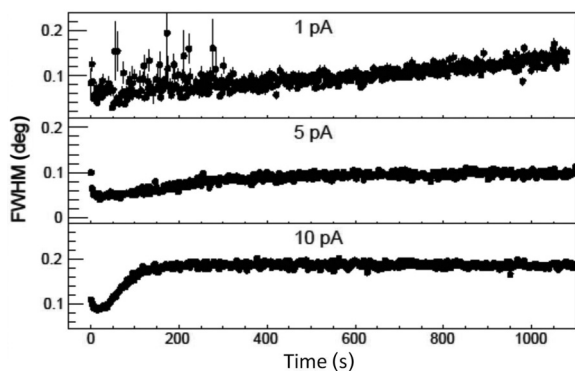


FIG. 4. Evolution of the FWHM of the transmitted beam for the conical-shaped capillary corresponding to Fig. 3 as a function of time (charge). The beam intensities are the same as in Fig. 3.

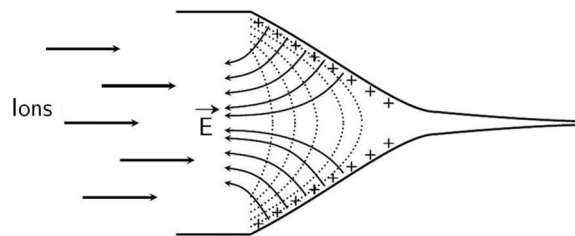


FIG. 5. Schematic of the cusp part of the funnel-shaped capillary showing the electric field and potential barrier that arise from the deposited charge. The solid lines correspond to electric-field lines, and the dotted lines correspond to equipotential surfaces.

Assuming the input beam is parallel, Fig. 5 shows a schematic of the charge deposited largely on the funnel-shaped part for the capillary at a tilt angle of 0° . Because of the low conductivity of the material, a large fraction of the incident ions striking the funnel-shaped part are expected to remain there as indicated. Then, due to the charge buildup, a potential barrier is formed by the high density of charge over a short length along the capillary axis. This potential barrier can completely block subsequent ions, even if their initial trajectory is directed to the opening of the capillary. The exact field is difficult to describe quantitatively because it depends on the shape of the funnel part and on the amount and distribution of charge on the wall. Nevertheless, the minimum potential needed to block the ions is 3 kV ($=27 \text{ keV} \div 9$) in this case. The charge needed for establishing such a barrier can be estimated if we assume that the deposited charge and the discharge speed are constant for different primary beam intensities. Based on the blocking for 5 and 10 pA in Fig. 2, the amount of deposited charge is obtained from the duration time of the irradiation multiplied by the injected beam current (Fig. 2) and is found to be about ~ 1000 pC. However, this barrier could be reduced by decreasing the taper angle of the capillary.

Such a blocking field is expected to be more efficient with the beam and capillary well aligned. In the tilted case, the beam strikes one side of the wall at a larger incident angle than the tilt angle and the other side at a smaller angle than the tilt angle. In the former case, an ion in the beam is more likely to be scattered by the asymmetric field and buried in the wall, whereas, for the latter case, the beam will be scattered less and, hence, is more likely to be guided and transmitted. Essentially, the blocking is attributed to the symmetric distribution of the charge deposition at the tilt angle of $\sim 0^\circ$, whereas, for nonzero tilt angles, the symmetry is broken, thereby leading to more stable ion transmission. This scenario was first proposed in Ref. [12].

Transmission for the conical capillary occurs continuously even for higher beam intensities up to at least 10 pA. This difference shows the importance of the capillary shape in the transmission and blocking of an ion beam. The reason for continuous transmission at 0° provided by the conical capillary is that the ion trajectory angle with the capillary wall is always smaller than the guiding angle. This is not the case for the funnel capillaries for which blocking occurs for lower beam intensities. However, for funnel or conical capillaries and even for cylindrical nanocapillary foils [5], barrier blocking can also occur with increasing tilt angle.

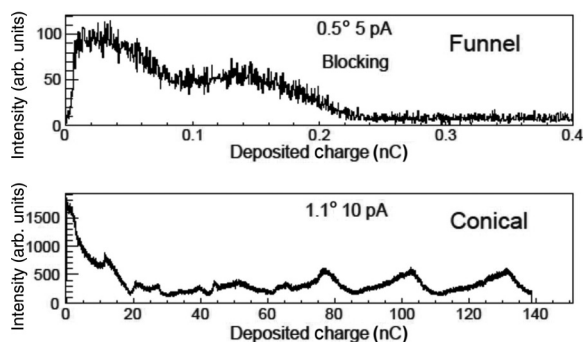


FIG. 6. Transmitted beam intensity evolution in arbitrary units for funnel- and conical-shaped capillaries measured as a function of deposited charge for tilt angles greater than zero. For the funnel-shaped capillary, the tilt angle is 0.5° (upper panel), and for the conical-shaped capillary, the tilt angle is 1.1° (lower panel).

Transmission and blocking for the funnel capillary at a tilt angle of 0.5° and 5 pA and transmission for the conical capillary at 1.1° and 10 pA, respectively, are shown in Fig. 6. For the funnel capillary (upper panel of the figure), transmission shows a slight blocking at about 0.1 nC (~ 20 s) before becoming fully blocked at ~ 0.25 nC (~ 50 s), whereas, the transmission lasted for ~ 400 s (2 nC) for 0° as shown in the upper panel of Fig. 2 for the same beam intensity. For the conical capillary at 1.1° with a beam intensity of ~ 10 pA (lower panel of Fig. 6), the beam is transmitted for a longer time and higher integrated charge, but several shifts of the intensity value indicate that charging and discharging cycles occur on the capillary walls. In the beginning, these cycles are chaotic, but after a deposited charge of 70 nC, a dynamic equilibrium is reached as shown by the observed oscillations. This behavior is similar to that recently reported in the case of ion transport between two insulating plates [17]. For the funnel capillary at a tilt angle of $\sim 1^\circ$, no beam was transmitted after waiting for 220 s with a beam intensity of ~ 1 pA. In contrast, for the conical capillary, transmission was observed up to a tilt angle of 1.8° with the ions being transmitted after a shorter delay time. Such a phenomenon can be attributed to the angle of the taper of the capillaries. As the tilt angle is increased, the angle between the capillary wall and the beam exceeds

the guiding angle sooner for the funnel capillary than for the conical capillary. Since the guiding angle for the glass surface is the same for both shapes, it can, therefore, be expected that the funnel capillary blocks the transmission first.

These results show the importance of the capillary shape for efficient ion transmission. A study to optimize the taper angle distribution is in progress.

To summarize, the transmission comparison of two different capillary shapes, so-called funnel and conical shapes, was presented for different injected ion beam intensities and tilt angles. It was found that the blocking effect for the funnel capillary happens after rather short charging times, whereas, transmission and guiding occurred continuously for the conical capillary. Blocking of the funnel capillary was attributed to a potential barrier that was established by charge collection at the funnel section of the specimen. The shape and height of the potential barrier depend on the injected intensity, taper angle, and tilt angle. The lower limit for the blocking intensity for the conical capillary could not be determined from our experiments since this limit was not reached for the beam intensities used. This value would be of interest to reveal further details of the transmission and guiding processes. Since the funnel capillary is already being utilized for several applications, the transmission properties of the conical capillary should be further studied for these same applications to see if improvements can be achieved [1,7,11,14,18–21]. Finally, these results show that the understanding of the guiding process in an insulating capillary must take into account not only the inner surface charging, but also the capillary shape which appears to be of importance.

The authors wish to thank the staffs of CIMAP and GANIL for their excellent technical support. C.L.Z. was supported by the International Graduate Scholarship Program (IGSP) from the China Scholarship Council. J.A.T. was supported by a grant from the Basse-Normandie region (Convention No. 11P01476) and from the European Union through its FEDER fund (Grant No. 32594). This work has been supported by the European Union as an Integrating Activity “Support of Public and Industrial Research Using Ion Beam Technology (SPIRIT)” under EC contract No. 227012.

- [1] T. Ikeda, Y. Kanai, T. M. Kojima, Y. Iwai, T. Kambara, Y. Yamazaki, M. Hoshino, T. Nebiki, and T. Narusawa, *Appl. Phys. Lett.* **89**, 163502 (2006).
- [2] N. Stolterfoht, J.-H. Bremer, V. Hoffmann, R. Hellhammer, D. Fink, A. Petrov, and B. Sulik, *Phys. Rev. Lett.* **88**, 133201 (2002).
- [3] H. F. Krause, C. R. Vane, and F. W. Meyer, *Phys. Rev. A* **75**, 042901 (2007).
- [4] H.-Q. Zhang, P. Skog, and R. Schuch, *Phys. Rev. A* **82**, 052901 (2010).
- [5] N. Stolterfoht, R. Hellhammer, B. Sulik, Z. Juhász, V. Bayer, C. Trautmann, E. Bodewits, and R. Hoekstra, *Phys. Rev. A* **83**, 062901 (2011).
- [6] R. J. Berezky, G. Kowarik, F. Aumayr, and K. Tökési, *Nucl. Instrum. Methods Phys. Res. B* **267**, 317 (2009).
- [7] A. Cassimi, L. Maunoury, T. Muranaka, B. Huber, K. R. Dey, H. Lebius, D. Lelièvre, J. M. Ramillon, T. Been, T. Ikeda, Y. Kanai, T. M. Kojima, Y. Iwai, Y. Yamazaki, H. Khemliche, N. Bundaleski, and P. Roncin, *Nucl. Instrum. Methods Phys. Res. B* **267**, 674 (2009).
- [8] Y. Yamazaki, *Phys. Scr. T* **73**, 293 (1997).
- [9] A. R. Milosavljević, G. Víkor, Z. D. Pěšić, P. Kolarž, D. Šević, B. P. Marinković, S. Mátéfi-Tempfli, M. Mátéfi-Tempfli, and L. Piraux, *Phys. Rev. A* **75**, 030901(R) (2007).
- [10] S. Das, B. S. Dassanayake, M. Winkworth, J. L. Baran, N. Stolterfoht, and J. A. Tanis, *Phys. Rev. A* **76**, 042716 (2007).
- [11] T. M. Kojima, D. Tomono, T. Ikeda, K. Ishida, Y. Iwai, M. Iwasaki, Y. Tatsuda, T. Matsuzaki, and Y. Yamazaki, *J. Phys. Soc. Jpn.* **76**, 093501 (2007); D. Tomono *et al.*, *ibid.* **80**, 044501 (2011).

- [12] R. Nakayama, M. Tona, N. Nakamura, H. Watanabe, N. Yoshiyasu, C. Yamada, A. Yamazaki, S. Ohtani, and M. Sakurai, *Nucl. Instrum. Methods Phys. Res. B* **267**, 2381 (2009).
- [13] T. Schweigler, C. Lemell, and J. Burgdörfer, *Nucl. Instrum. Methods Phys. Res. B* **269**, 1253 (2011).
- [14] M. J. Simon, M. Döbeli, A. M. Müller, and H. A. Synal, *Nucl. Instrum. Methods Phys. Res. B* **273**, 237 (2012).
- [15] A. Cassimi, T. Ikeda, L. Maunoury, C. L. Zhou, S. Guillous, A. Mery, H. Lebius, A. Benyagoub, C. Grygiel, H. Khemliche, P. Roncin, H. Merabet, and J. A. Tanis *Phys. Rev. A* **86**, 062902 (2012).
- [16] <http://root.cern.ch/drupal/>
- [17] T. Ikeda, Y. Iwai, T. M. Kojima, S. Onoda, Y. Kanai, and Y. Yamazaki, *Nucl. Instrum. Methods Phys. Res. B* **287**, 31 (2012).
- [18] Y. Iwai, T. Ikeda, T. M. Kojima, Y. Yamazaki, K. Maeshima, N. Imamoto, T. Kobayashi, T. Nebiki, T. Narusawa, and G. P. Pokhil, *Appl. Phys. Lett.* **92**, 023509 (2008).
- [19] J. Hasegawa, S. Jaiyen, C. Polee, N. Chancow, and Y. Oguri, *J. Appl. Phys.* **110**, 044913 (2011).
- [20] T. Nebiki, T. Yamamoto, T. Narusawa, M. B. H. Breese, E. J. Teo, and F. Watt, *J. Vac. Sci. Technol. A* **21**, 1671 (2003).
- [21] N. Fujita, K. Ishii, and H. Ogawa, *Nucl. Instrum. Methods Phys. Res. B* **269**, 1023 (2011).